Electrochemical investigation on the redox chemistry of niobium in LiCl-KCl-KF-Na2O melts

Gillesberg, Bo; Bjerrum, Niels; Barner, Jens H. Von; Lantelme, Frédéric

Published in:
Journal of The Electrochemical Society

Link to article, DOI:
10.1149/1.1838029

Publication date:
1997

Document Version
Publisher's PDF, also known as Version of record

Electrochemical Investigation on the Redox Chemistry of Niobium in LiCl-KCl-KF-Na_2O Melts

Bo Gillesberg, Niels J. Bjerrum,* and Jens H. von Barner

Department of Chemistry, Technical University of Denmark, DK-2800 Lyngby, Denmark

Frédéric Lantelme*

Laboratoire d'Electrochimie URA 430 CNRS, Université Pierre et Marie Curie, F-75252, Paris Cedex 05, France

ABSTRACT

The system LiCl-KCl-KF-1 mole percent K_2NbF_7 (molar ration $F^-/Nb = 8$) has been investigated in the temperature range 370 to 725°C by cyclic and square wave voltammetry. In the temperature range from 370 to 520°C Nb(V) was reduced to Nb(III) in two reversible steps: Nb(V) → Nb(IV) → Nb(III). At these temperatures subvalent halides of niobium were formed at more negative potentials. At temperatures above 660°C metallic niobium was formed during reduction. When oxide (molar ratio $O^{2-}/Nb = 1.1$) was introduced in the melt at 725°C only minor changes were observed in the voltammograms. It is suggested that oxide addition mainly leads to precipitation of oxide containing compounds.

Introduction

LiCl-KCl melts are possible alternatives to fluoride melts as molten salt baths for electrochemical plating of corrosion resistant layers of niobium metal. Although all fluoride melts, *e.g.*, LiF-NaF-KF eutectic melts (FLINAK), seem to fulfill most of the technical demands to produce high quality surface layers of niobium,[1,2] such melts are extremely difficult to handle due to their corrosive nature. Further they may cause environmental problems after use. Therefore considerable efforts have been made to develop processes based on chloride[3-6] and mixed chloride-fluoride baths.[3,5,7-11] However in all chloride melts formation of unwanted lower valent species of niobium often accompany the electrolytic deposition of the metal,[3-5] whereas mixed chloride-fluoride melts seem to be more promising.[7,8]

NaCl-KCl melts, with addition of K_2NbF_7 as niobium source, are among the best investigated of the latter category. In fact coherent and reasonable smooth layers of niobium metal have been obtained from such melts.[7] Although NaCl-KCl is the cheapest choice of solvent, the rather high melting point (approximately 700°C) of these mixtures may be a disadvantage. LiCl-KCl offers a wider range of liquidus temperatures, *e.g.*, the melting point of the eutectic mixture is as low as 354°C.

At high temperatures (> approximately 600°C) the reduction of Nb(V) is reported to proceed according to

$$Nb(V) + 5e^- \rightarrow Nb(IV) + 4e^- \rightarrow Nb(metal) \qquad [1]$$

both in mixed chloride/fluoride melts[7,8,10,12] (with the molar ratio of fluoride to niobium $F/Nb \geq 7$), and in fluoride melts.[13-15] This conclusion has mainly been drawn from experiments performed by cyclic voltammetry (CV).

At lower temperatures most work has been performed on all chloride systems such as chloroaluminate[3,16] and LiCl-KCl melts.[5,17,18] The situation seems to be rather complicated and a number of different reduction paths for Nb(V) have been proposed. Only a few publications deal with the influence of oxide[5,16,17] or fluoride[3,5] at low temperatures. No work seems to have been performed on the niobium redox chemistry in LiCl-KCl melts with fluoride or oxide additions at temperatures above 550°C.

It was therefore decided to investigate the redox chemistry of niobium in LiCl-KCl-KF melts as a function of the temperature. In our experiments both CV and square wave voltammetry (SWV) have been applied in order to overcome problems with merging redox waves. Further we included measurements on melts with added oxide, since the presence of oxide often influences the possibility of getting niobium deposited in a reasonable pure quality.[2,13,19]

* Electrochemical Society Active Member.

Experimental

The solvent (anhydrous eutectic LiCl-KCl mixture) was prepared in the following way: analytical grade LiCl and KCl from Merck were previously dried at 140°C for 2 days. Subsequently the salts were weighed, mixed, and placed in the dehydration apparatus described in details elsewhere.[20] Gaseous hydrogen chloride (Gerling Holz; 99.995%) was passed through the salts for approximately 45 min, while they were heated to a temperature approximately 25°C beyond the melting point. The gas flow was retained 15 min after the salts were melted. Then nitrogen (Air Liquide, 99.8%) was led through the melt for 10 min to remove dissolved HCl. Both gasses were dried in columns filled with P_2O_5 before entering the dehydration apparatus. The melt was subsequently filtered and allowed to solidify in a quartz ampul, which was sealed under vacuum. Alternatively the salts were dehydrated directly in the setup used for the electrochemical experiments according to the following procedure: the salts were mixed in a vitreous carbon crucible which was then evacuated overnight at 130°C. The salts were then treated with chlorine (Air Liquide N27) during heating to the melting point and thereafter for 15 min in the molten state.

The alkali metal fluorides (Merck, analytical grade) were purified by recrystallization from molten state under argon atmosphere followed by mechanical separation as described previously.[21] K_2NbF_7 was prepared by mixing hot solutions of KF (Merck, analytical grade) and Nb_2O_5 (Cerac, 99.95%). The product (precipitate) was then recrystallized in 40% hydrofluoric acid.[13] NaO_2 was formed by heating Na_2O_2 under vacuum as earlier reported.[13] All handling and weighing of the chemicals were carried out in a glove box with a dry argon atmosphere (dew point approximately −45°C).

The voltammograms were generated by the means of a potentiostat (EG&G Princeton Applied Research Model 273 or Tacussel PRT 20-10X). The square wave voltammograms were obtained with a symmetrical square wave form (*i.e.*, the forward and reverse pulses were of equal duration) and the current was measured just before switching the signal. These voltammograms could be resolved with a computer program (PeakFit™ from Jandel Scientific) that fitted the experimental curves according to a Gaussian procedure. All the experiments were conducted under argon atmosphere (≥99.99%) either by flow or a gauge pressure of 0.2 bar. The furnaces and experimental procedures have been described in detail elsewhere.[5,13]

Electrode setup: either a platinum wire (quasi-reference electrode) or a Ni^{2+}/Ni reference electrode were used in the experiments. The Ni^{2+}/Ni reference electrode consisted of a nickel wire immersed in an inner melt [LiCl-KCl with 1 mole percent (m/o) KF and 1 m/o $NiCl_2$ added]. The inner

melt was separated from the bulk solution by a BN diaphragm. The counterelectrode (platinum or vitreous carbon) had an area of minimum 2 cm^2. In all the experiments a platinum indicator electrode was used.

Results and Discussion

As mentioned in the experimental section both a Ni^{2+}/Ni-electrode and platinum metal have been applied as reference electrodes in our experiments. To simplify the discussion all potentials are referred *vs.* the Ni^{2+}(1 m/o $NiCl_2$)/Ni reference electrode.

Cyclic voltammetry.—Figure 1 shows a typical voltammogram obtained at 725°C of an eutectic LiCl-KCl melt with K_2NbF_7 and KF (molar ratio F/Nb = 7.9) added. The anodic limit is due to oxidation of the indicator electrode (platinum). Two reduction waves R_1 (0.24 V) and R_2 (−0.3 V) followed by a strong reduction wave R_3 (−0.45 V) appear in the voltammogram. R_3 is accompanied by an oxidation wave Ox_3 at −0.3 V. The reduction waves R_1 and R_2 are not very obvious in Fig. 1 but appear distinctly in Fig. 2 where the ordinate scale (current) has been magnified. On this figure it can be seen that R_1 and R_2 are coupled to the oxidation waves Ox_1 (0.4 V) and Ox_2 (0.2 V), respectively.

R_1/Ox_1.—In the scan range 0.5 to 20 V/s the peak potential of R_1 remained constant, and the peak current was proportional to the square root of the scan rate. Obviously R_1/Ox_1 is due to a reversible process. The difference between the peak and half-peak potential ($E_p - E_{p/2}$) of R_1 was 0.17 V. When the equation

$$| E_p - E_{p/2} | = 2.2RT/nF \quad [2]$$

that is valid for reversible reactions,[22] is applied, an n value of 1.1 is obtained.

As can be seen from Fig. 1 and 2 the oxidation wave Ox_1 is overlapped by Ox_2 and the current due to oxidation of the Pt working electrode. Therefore exact values of the peak potential of Ox_1 could not be obtained at high temperatures (>600°C). However at lower temperatures (in the range from 370 to 520°C) Ox_1 is to a lesser extent overlapped by other waves, as can be seen in Fig. 3A-C. From these voltammograms the number of electrons involved was calculated by the equation[22]

$$E_p^a - E_p^c = 2.2RT/nF \quad [3]$$

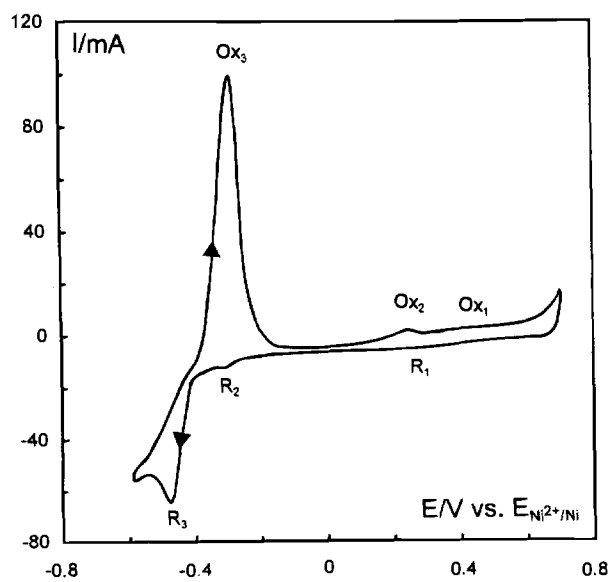

Fig. 1. Cyclic voltammogram at 725°C of K_2NbF_7 (1.1 m/o) dissolved in eutectic LiCl-KCl melt with KF (1.0 m/o) added. Scan rate: 0.5 V/s. Platinum working (0.024 cm^2), counter- and reference electrodes.

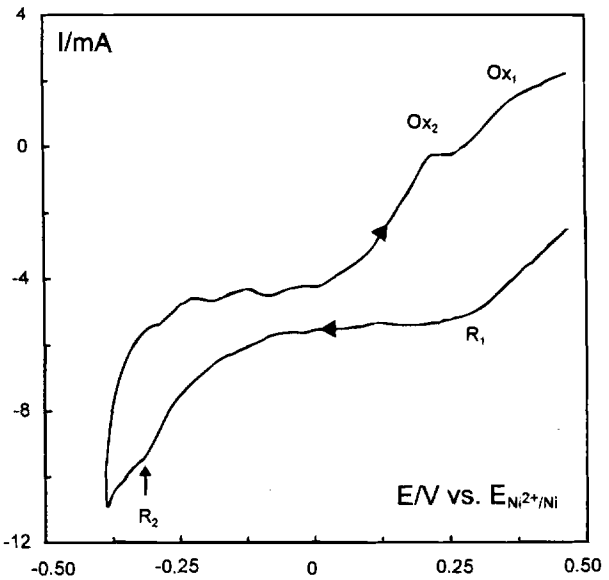

Fig. 2. Cyclic voltammogram at 725°C of K_2NbF_7 (1.1 m/o) dissolved in eutectic LiCl-KCl melt with KF (1.0 m/o) added. Scan rate: 0.5 V/s. Platinum working (0.024 cm^2), counter- and reference electrodes.

where E_p^a and E_p^c are the anodic and cathodic peak potential, respectively. The calculations gave n values between 0.8 and 1.0. Thus we conclude that one electron is transferred in the R_1/Ox_1 redox reaction corresponding to the equation

$$Nb(V) + e^- \leftrightarrow Nb(IV) \quad [4]$$

This redox process has previously been reported to take place in all chloride,[3-6,9,16,17,23] all fluoride,[13-15,21] and mixed chloride fluoride[3,5,7,8,10,19] melts.

R_2/Ox_2.—R_2 appears to be weak but relatively sharp (Fig. 1 and 2). The wave potential of R_2 changed markedly toward more negative potentials when the scan rate was increased. Furthermore the separation between the anodic and the cathodic peak potential is quite large (0.5 V). We probably deal with a process that involves solid-state diffusion. The fact that R_2/Ox_2 is only observed at high temperatures (> 650°C) probably indicates the formation of a Nb-Pt alloy. Such alloys are known from the Nb-Pt phase diagram[24] and have previously been reported during reduction of Nb(V) in NaCl-KCl melts at 900°C.[25] Further electrolysis was performed at a constant potential slightly more negative than R_2. A platinum substrate was used as cathode. A gray deposit, which was insoluble in water was formed. A scanning electron microscope (SEM) investigation showed that the plate was covered by a thin surface layer. An electron disperse x-ray analysis (EDX) of the layer gave signals from platinum and niobium. The average niobium to platinum atomic ratio was measured to be 0.3. These results suggest formation of a Nb-Pt alloy.

R_3/Ox_3.—R_3 is the strongest reduction wave in Fig. 1. Compared to R_1 the current involved in R_3 is considerably higher, indicating that more than one electron takes part in the process. Ox_3 has the shape of a stripping peak, suggesting that a solid product is formed at the working electrode during reduction. The observed pattern with a steep reduction wave (R_3) situated at a potential approximately 0.7 V more negative than the $Nb_{V/IV}$ reduction (R_1) is similar to observations at temperatures near 700°C in both FLINAK and NaCl-KCl melts with K_2NbF_7 added.[7,21] In both cases the reduction product was identified to be metallic niobium. To investigate whether this is the case also in LiCl-KCl, electrolysis was performed at a constant potential corresponding to that of R_3. Molybdenum was chosen as cathode material since it does not form alloys

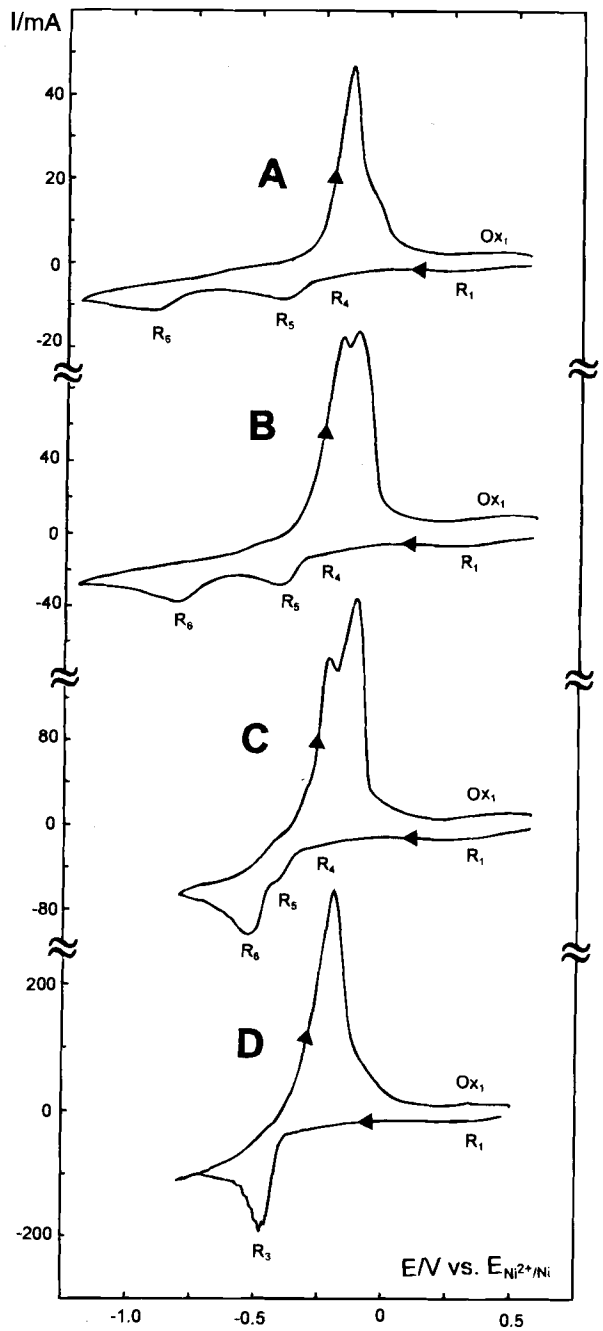

Fig. 3. Cyclic voltammograms at different temperatures of K_2NbF_7 (1.0 m/o) dissolved in eutectic LiCl-KCl melts with KF (1.0 m/o) added. Scan rate: 0.5 V/s. Platinum working electrode (0.047 cm^2), vitreous carbon counterelectrode, and $NiCl_2$(1 m/o)/Ni reference electrode. Temperatures: A, 370°C; B, 450°C; C, 520°C; D, 660°C.

with niobium. A powdery gray layer covered by a black crust, was obtained. We have not been able to identify the nature of the black crust. However it could be dissolved in ethanol, resulting in a yellow-green solution. It is known that subvalent niobium species have dark colors and that some of these can be dissolved in ethanol to form olive solutions.[3,26] The gray layer beneath consisted of nodules that were insoluble both in water and alcohol. Electrolytically deposited niobium metal from FLINAK melts has been reported[13] to have a very similar morphology as we observe. Further an EDX analysis of the nodules showed signals from niobium. Consequently we conclude that metallic niobium is formed during the R_3 reduction. However it seems that the deposit also involves subvalent halides.

Influence of the temperature.—Figure 3 shows how the voltammograms change as a function of temperature in the range 370 to 660°C. Both the cathodic and anodic wave of R_1/Ox_1 are slightly displaced toward more negative values, when the temperature is lowered. The standard potential E^0 of a reversible reaction can be calculated from the equation[22]

$$E^0 = 0.5\ (E_p^a - E_p^c) \qquad [5]$$

As a result the following equation describes the temperature dependence of the Nb(V)/Nb(IV) redox couple

$$E^0_{V/IV} = (0.26 + 2.3 \cdot 10^{-4} \cdot T/°C)\ V \qquad [6]$$

in the temperature region from 370 to 520°C.

Furthermore two strong reduction waves (R_5 and R_6) are observed in Fig. 3A-C. The peak potential of R_5 (−0.4 V) is almost independent of the temperature up to 520°C whereas R_6 shifts toward positive potentials with increasing temperature, *e.g.*, from a wave potential of −0.9 V at 370°C (Fig. 3A) to −0.5 V at 520°C (Fig. 3C). As the temperature reaches 660°C (Fig. 3D) R_5 and R_6 merge into one wave, R_3. Thus the voltammogram is now very similar to the one previously recorded at 725°C (Fig. 1). Besides the more obvious reductions described above, it can further be seen that a supplementary reduction R_4 occurs in the region −0.1 to −0.35 V. Two strong oxidation waves in the region 0 to −0.25 V are apparent in Fig. 3. The one at the most positive potential is seen as a shoulder at the lowest temperature (370°C) and seems to grow with increasing temperature.

In order to clarify the correspondence between oxidation and reduction waves, experiments with changing cathodic reverse potential were performed. The resulting voltammograms can be seen in Fig. 4. It appears that R_5 is accompanied by a weak oxidation wave Ox_5 around −0.2 V. This wave is obviously not a stripping peak, which implies that the reduction product of R_5 is soluble. The correspondence between R_6 (−0.8 V) and the stripping peak Ox_6 (−0.3 V) appears clearly from the voltammogram where the potential is reversed at a potential slightly more negative than R_6 (dotted line). For even more negative reverse potentials a second stripping wave Ox_6' (approximately −0.1 V) shows up.

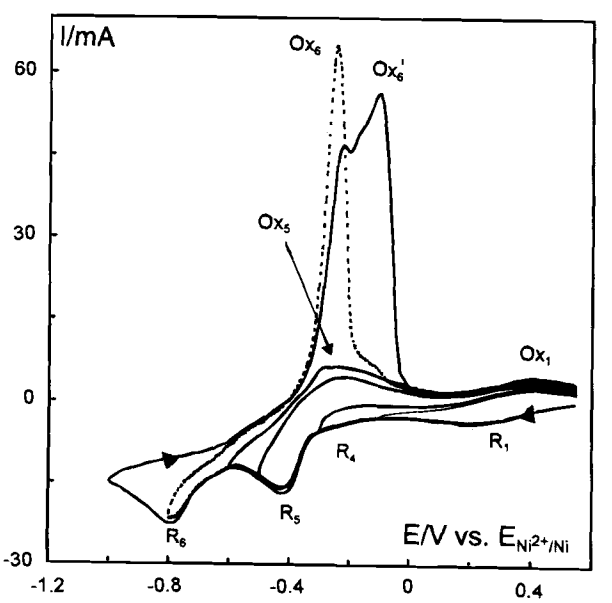

Fig. 4. Cyclic voltammograms at 450°C with different cathodic reverse potentials of K_2NbF_7 (1.0 m/o) dissolved in eutectic LiCl-KCl melts with KF (1.0 m/o) added. Platinum working electrode (0.047 cm^2), vitreous carbon counterelectrode, and $NiCl_2$(1 m/o)/Ni reference electrode. Scan rate: 0.5 V/s.

R_4.—At the scan rate applied in Fig. 4 (0.5 V/s) it was difficult to obtain specific information about R_4, since the wave was partly overlapped by the following reduction wave (R_5). However, it was possible to separate R_4 and R_5 when the scan rate exceeded 1 V/s, since R_5 shifted in negative direction. R_4 now appeared as a distinct wave (Fig. 5). For scan rates between 1 and 20 V/s R_4 and Ox_4 was situated at constant potentials of −0.30 and −0.16 V, respectively. Thus the redox couple R_4/Ox_4 seems to be due to a reversible reaction. It appears that the difference in the wave potentials ($E_p^a - E_p^c$) is 140 mV. If Eq. 3 is applied an n value of 1.1 can be calculated. Probably one electron is involved in the process R_4/Ox_4. Since we, from what previously has been said, can assume that Nb(V) has been reduced to Nb(IV) in a step previous to the R_4 reduction, it is most likely that R_4 is due to a reversible reduction of Nb(IV) to Nb(III) according to the equation

$$\text{Nb(IV)} + e^- \leftrightarrow \text{Nb(III)} \qquad [7]$$

As we shall see in a later paragraph this hypothesis is supported by our square wave experiments. At 450°C the standard potential for the Nb(IV)/Nb(III) reaction was calculated from Eq. 5 to −0.23 V. To judge from the voltammogram recorded at 660°C (Fig. 3D) and 725°C (Fig. 1) R_4 may still be present as a prewave to R_3 even at high temperatures.

The Nb(IV)/Nb(III) reduction is known to take place over a wide temperature range in all chloride melts such as LiCl-KCl, NaCl-KCl and CsCl-NaCl melts.[5,6,23] In addition previous work[5] also showed the presence of the Nb(IV)/Nb(III) redox pair in a LiCl-KCl melt at 450°C with fluoride added (F^-/Nb up to 8).

R_5.—We have further investigated the influence of the scan rate on the voltammogram at 450°C with cathodic reverse potential just beyond the one of R_5. The peak potential of R_5 *vs.* the logarithm of the scan rate is shown in Fig. 6.. Three regions appear. At low scan rates (between 5 and 50 mV/s) the peak potential is constant (−0.41 V) indicating a reversible reaction. For scan rates between 50 mV/s and 1 V/s a nonlinear change is observed. At scan rates above 1 V/s the curve again becomes linear suggesting that we now deal with an irreversible reduction. In the latter case the number of electrons taking part in the reaction can be estimated from the following equation[22]

$$E_p^c = K - (2.3\,RT)/(2\alpha nF)\log \nu \qquad [8]$$

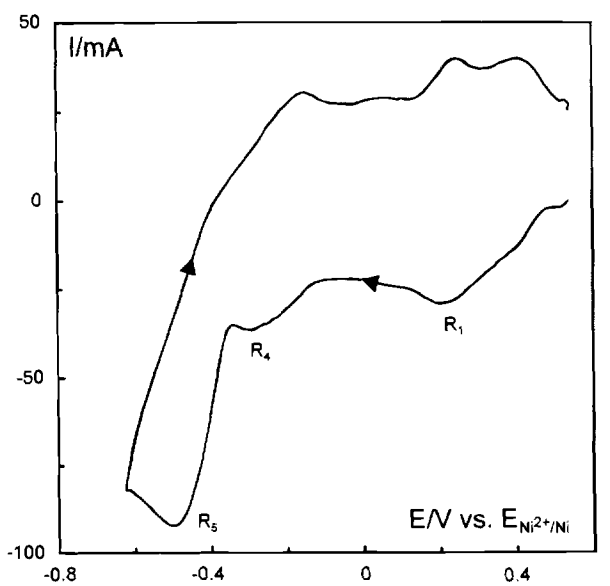

Fig. 5. Cyclic voltammogram at high scan rate of eutectic LiCl-KCl melt at 450°C with K_2NbF_7 (1.0 m/o) and KF (1.0 m/o) added. Platinum working electrode, vitreous carbon counterelectrode, and $NiCl_2$ (1 m/o)/Ni reference electrode. Scan rate: 20 V/s.

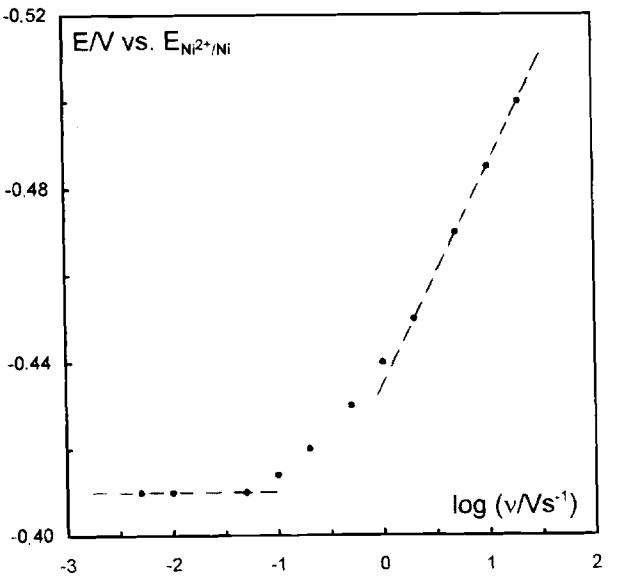

Fig. 6. Variation of the peak potential of R_5 *vs.* the logarithm of scan rate at 450°C. See text.

where K is a constant, α the transfer coefficient, and ν is the scan rate. From Eq. 8 and the slope of the curve a value of $\alpha n = 1.6$ can be calculated. In the case of redox reactions proceeding in solution it is normally safe to assume,[22] that α has a value between 0.4 and 0.6. Under this assumption we obtain an n value of approximately 3 for R_5.

As previously mentioned Eq. 2 can be used to estimate the number of electrons when the reaction is reversible. However R_4 overlaps R_5 in the range −0.2 to −0.3 V implying that a reliable value of the half-wave potential of R_5 cannot be obtained from the voltammograms in Fig. 3 or 4. A technique[27] where a constant potential slightly below the peak potential of the prewave is applied for a period may overcome this problem. In this way the current due to the preceding reduction is minimized as it appears from the Cottrell equation. Thus an initial potential of −0.30 V was applied for 10 s before the voltammograms were recorded. The result can be seen in Fig. 7 (dotted line). By comparison with the voltammogram under normal condition (full line) it is obvious that the current due to R_4 is eliminated to a reasonable extent. We can now estimate $|E_p - E_{p/2}|$ for R_5 to be 60 mV. This corresponds to an n value of 2.3. Thus considering this result and the n value (approximately 3) obtained from Fig. 6 (irreversible conditions) it seems like two or three electrons are involved in the process R_5/Ox_5. Further the standard potential $E^0_{R_5/Ox_5}$ was calculated from the voltammograms in the reversible region (Eq. 5) to −0.35 ± 0.02 V.

Since Ox_5 is not a stripping peak it is likely that R_5/Ox_5 only involves soluble species. A number of lower valent niobates are reported in the literature. Among them clusters containing Nb_3^{8+} are known to exist in soluble form in chloride media.[3,26,28,29] Thus R_5 could be due to formation of Nb_3^{8+} by reduction of Nb(III) in a two or three electron step

$$3n\ Nb^{3+} + ne^- \rightarrow n\ Nb_3^{8+}\ (n = 2 \text{ or } 3) \qquad [9]$$

In previous work[5] on the redox behavior of niobium in LiCl-KCl melts (without fluoride added) no wave corresponding to R_5 was observed. An attempt to investigate melts with fluoride added at potentials corresponding to our R_5 region was impeded by passivation of the vitreous carbon working electrode. Thus no definite conclusion could be made.[5]

R_6.—In Fig. 4 a reduction wave R_6 is observed near the cathodic limit of the voltammograms (−0.8 V). This wave seems to correspond to two oxidation waves Ox_6 and Ox'_6. These have the shapes of stripping waves indicating that

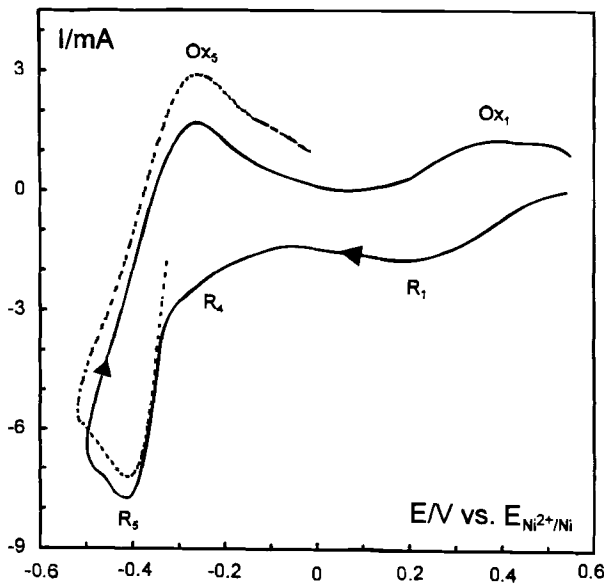

Fig. 7. Cyclic voltammograms (see text) at 450°C of eutectic LiCl-KCl melt with K_2NbF_7 (1.0 m/o) and KF (1.0 m/o) added. Scan rate: 50 mV/s. Platinum working electrode, vitreous carbon counterelectrode, and $NiCl_2$(1 m/o)/Ni reference electrode. Full line: normal conditions. Dotted line: initial potential of −0.3 V applied for 10 s before recording.

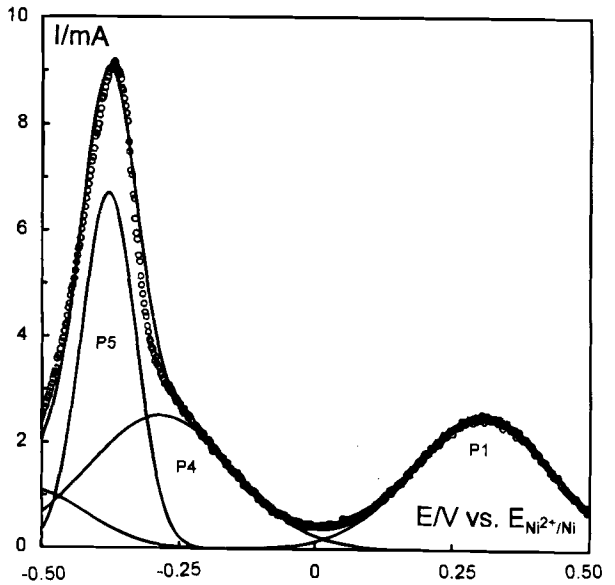

Fig. 8. Square wave voltammogram at 450°C of K_2NbF_7 (1.0 m/o) dissolved in eutectic LiCl-KCl melt with KF (1.0 m/o) added. Scan rate: 0.1 V/s, frequency: 50 Hz, square wave amplitude: 15 mV. Platinum working electrode, vitreous carbon counterelectrode, and $NiCl_2$ (1 m/o)/Ni reference electrode. Dotted line: measured current. Full lines: simulated waves.

two solid products are formed in the potential region near R_6. It thus appears that the R_6 wave could be due to two overlapping waves. An electrolysis at constant potential (−0.7 V) was subsequently performed in an attempt to identify the reduction products formed at 450°C. A gray deposit was obtained. However, it was not possible to identify the nature of the products by x-ray diffraction. It was observed that the diffractogram changed with time when the sample was exposed to the atmosphere (probably due to reaction with water vapor). The deposit was partly soluble in alcohol. This solution was olive-brown.

The pattern with a broad reduction wave and two corresponding oxidation peaks is very similar to previous observations in LiCl-KCl melts[5] at 450°C. In this case electrolysis at potentials slightly more positive than the peak potential of the reduction wave resulted in formation of subvalent niobium species. Further metallic niobium was formed when the deposition potential was displaced toward potentials more negative than the peak potential. Thus it seems likely insoluble subvalent niobates are also formed during reduction when fluoride is present in the melt.

Square wave voltammetry (SWV).—SWV[30-32] has proved to be a useful method to investigate redox reactions with overlapping waves. In the case of reversible processes the peaks are Gaussian shaped and the peak potentials are equal to the half-potentials ($E_{1/2}$) of the redox processes.[31] In our case we found it especially interesting to apply this method to the redox couples R_4/Ox_4 and R_5/Ox_5 since overlapping of the reduction waves occurred in the cyclic voltammograms. It was possible to resolve the obtained voltammogram into individual Gaussian curves (P1, P4, and P5) by a peak separation computer software as it appears in Fig. 8. Obviously P1, P4, and P5 correspond to the redox couples R_1/Ox_1, R_4/Ox_4, and R_5/Ox_5 previously observed by cyclic voltammetry (Fig. 4). P1 and P4 have similar shapes and heights whereas P5 are slimmer and two to three times more intensive than P1 and P4. The wave characteristics of the simulated waves are seen in Table I. A rough estimate of the number of electrons involved can be obtained from the peak height (*i.e.*, the peak current), which is almost proportional to n.[31] It seems that the same number of electrons are involved in P1 and P4 whereas more electrons are transferred in P5. A more exact evaluation of the number of electrons involved can be calculated from the half-peak widths ($W_{1/2}$). The half-peak widths depend on the temperature, the number of electrons involved, and the applied square wave amplitude.

Christie *et al.*[31] have calculated values of $W_{1/2}$ of reversible reactions for square wave amplitudes (E_{SW}) up to $n \cdot E_{SW}$ = 50 mV. In Table II the theoretical expressions for $W_{1/2}$ are shown for different values of n when a square wave amplitude of 15 mV is applied (as in our work). If the values of the half-peak widths (Table I) are considered n values of 0.8 are obtained for both P1 and P4. For P5 n can be calculated to 2.2 or 2.7 assuming n = 2 or n = 3, respectively. These results agree well compared to those previously obtained by CV.

Influence of oxide.—In Fig. 9 voltammograms of melts without and with Na_2O added are compared. In the voltammogram with oxide added (Fig. 9B) a small additional reduction wave R_7 appears approximately 0.1 V more negative than R_3.

The changes in the shape of the voltammograms when oxide is added are less pronounced than in FLINAK or NaCl-KCl melts containing K_2NbF_7. In those solvents the

Table I. Peak potential (E_p), peak height (I_p), and half-wave width ($W_{1/2}$) of the peaks calculated from the square wave voltammogram at 450°C (Fig. 8).

Peak	E_p (V)	I_p (mA)	$W_{1/2}$ (mV)
P1	0.30	2.4	300
P4	−0.28	2.4	312
P5	−0.37	6.8	116

Table II. Theoretical half-wave width ($W_{1/2}$) as a function of the number of electrons. Square wave amplitude: 15 mV.

n	$n \cdot E_{SW}$ (mV)	$W_{1/2}$ (mV)
1	15	3.88 RT/nF
2	30	4.04 RT/nF
3	45	5.02 RT/nF

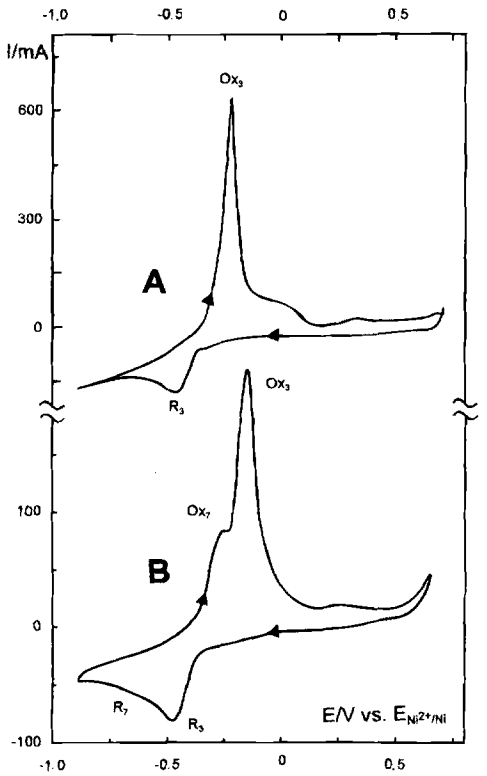

Fig. 9. Cyclic voltammograms at 725°C without and with Na_2O added of K_2NbF_7 (1.0 m/o) dissolved in LiCl-KCl-KF melt (F/Nb = 7.9). Scan rate: 5 V/s. Platinum working (0.24 cm²), counter- and reference electrodes. Molar ratios O/Nb: A: 0, B: 1.08.

wave corresponding to R_3 has disappeared and is replaced by a wave more negative (0.2 V).[21,33] Raman spectroscopic investigations on those melts show a nearly quantitative formation of oxo complexes when oxide is added to the melts,[34] *i.e.*, the equilibrium

$$NbF_7^{2-} + O^{2-} \leftrightarrows NbOF_n^{(n-3)-} + (7 - n)F^- \quad [10]$$

is shifted to the right. In our case where LiCl-KCl-KF is used as the solvent the effect of the oxide addition is expressed to a lesser extent since we still observe R_3 at an O/Nb molar ratio slightly above one (1.1). The reason for this could be precipitation of a Nb(V) oxo compound. Thermodynamic calculations[17] on niobium dissolved in LiCl-KCl support this view since $LiNbO_3$ obviously forms at low pO^{2-} (*i.e.*, high oxide content). In the voltammogram in Fig. 9B a further oxidation wave Ox_7 appears besides the wave due to oxidation of niobium metal (Ox_3). Obviously a second deposit is formed at the electrode during reduction. One could suggest that a subvalent oxide-containing compound is formed. However, this wave is very weak and the amount of material deposited is small, which makes it difficult to identify the reduction product.

Conclusion

The redox chemistry of K_2NbF_7 dissolved in LiCl-KCl-KF melts (molar fluoride to niobium ratio F/Nb = 8.0) has been investigated in the temperature range 370 to 725°C. At low temperatures (370 to 520°C) cyclic voltammetry and square wave voltammetry show that Nb(V) is reduced to Nb(III) in two reversible steps

$$Nb(V) + e^- \rightleftarrows Nb(IV) + e^- \leftrightarrow Nb(III) \quad [11]$$

The standard potential $E^0_{V/IV}$ was found to vary linearly with the temperature according to $(0.26 + 2.3 \cdot 10^{-4}\ T/°C)$ V [*vs.* Ni^{2+} (1 m/o $NiCl_2$)/Ni]. At moderate scan rates (less than 1 V/s) the reduction of Nb(IV) to Nb(III) appeared as a prewave in the voltammograms in the region −0.2 to −0.3 V. The standard potential $E^0_{IV/III}$ was −0.23 V at 450°C. The wave due to formation of Nb(III) is less pronounced at higher temperatures. A two-step reduction of Nb(V) to Nb(III) has also been observed in chloride melts without fluoride additions in a wide temperature range.[5,6,23] It would be interesting to compare our results with electrochemical experiments in all fluoride melts, a situation where only fluoro complexes can be formed, at low temperatures (*i.e.*, below 600°C). However only investigations at higher temperatures on such melts appear in the literature.[13-15]

In the temperature range from 370 to 520°C two strong reduction waves appear at more negative potentials than the Nb(IV)/Nb(III) reduction wave. The first (around −0.4 V) is due to formation of a soluble product. We suggest formation of Nb_3^{8+} as a possibility. The second wave (around −0.8 V) involves formation of two solid products (probably a subvalent niobium cluster compound and niobium metal). When the temperature exceeded 660°C the two reduction waves merged into one wave due to niobium metal formation.

Knowledge about the formation of niobium complexes could be a key for understanding the different redox behavior at low and high temperatures. Unfortunately the electrochemical measurements applied in our work are not suitable for clarifying the complex formation. So the question whether we deal with fluoro, mixed fluoro/chloro, or chloro complexes at low temperatures remains open. The problem may be solved by spectroscopic measurements, which have previously[33] been shown to be useful for clarifying the situation in mixed chloride/fluoride media at high temperatures.

Only small changes were observed in the voltammograms when oxide was added to the melt at 725°C. The wave due to metal deposition from niobium halide complexes was still the strongest wave after oxide had been introduced in an amount equal to O/Nb = 1.1. Consequently the formation of soluble oxo complexes in LiCl-KCl melt is less pronounced than in FLINAK and NaCl-KCl melts with K_2NbF_7 added. Precipitation of niobates, *e.g.*, $LiNbO_3$, may take place upon oxide addition to niobium(V) containing LiCl-KCl melts.

Acknowledgment

This work has been performed in the frame of a CNRS (France)-SNF (Denmark) exchange program, which we acknowledge for financial support.

Manuscript submitted March 31, 1997; revised manuscript received June 24, 1997.

The Technical University of Denmark assisted in meeting the publication costs of this article.

REFERENCES

1. G. W. Mellors and S. Senderoff, U.S. Pat. 3,444,058 (1969).
2. J. H. von Barner, E. Christensen, and N. J. Bjerrum, Eur. Pat. 578605 (1994).
3. K. D. Sienerth, E. M. Hondrogianniz, and G. Mamantov, *This Journal*, **141**, 1762 (1994).
4. I. Elizanova, E. Polyakov, and L. Polyakova, *Mater. Sci. Forum*, **73-75**, 393 (1991).
5. F. Lantelme, A. Barhoun, and J. Chevalet, *This Journal*, **140**, 324 (1993).
6. C. Rosenkilde and T. Østvold, *Acta Chem. Scand.*, **49**, 85 (1995).
7. A. Barhoun, Y. Berghoute, and F. Lantelme, *J. Alloys Compd.*, **179**, 241 (1992).
8. F. Lantelme and Y. Berghoute, *This Journal*, **141**, 3306 (1994).
9. M. Chemla and V. Grinivich, *Bull. Soc. Chim. Fr.*, 853 (1973).
10. A. Khalidi, P. Taxil, B. Lafage, and A. P. Lamaze, *Mater. Sci. Forum*, **73-75**, 421 (1991).
11. V. I. Konstantitov, E. G. Polyakov, and P. T. Stangrit, *Electrochim. Acta*, **26**, 445 (1981).
12. Z. Alimanova, E. Polyakov, L. Polyakova, and V. Kremenetskiy, *J. Fluorine Chem.*, **59**, 203 (1992).
13. E. Christensen, X. Wang, J. H. von Barner, T. Østvold, and N. J. Bjerrum, *This Journal*, **141**, 1212 (1994).

14. P. Taxil and J. Mahenc, *J. Appl. Electrochem.*, **17**, 261 (1985).
15. Z. Qiao and P. Taxil, *ibid.*, **15**, 259 (1985).
16. I. W. Sun and C. L. Hussey, *Inorg. Chem.*, **28**, 2731 (1989).
17. G. S. Picard and P. Bocage, in *Proceedings of 8th International Symposium on Molten Salts*, R. J. Gale, G. Blomgren, and H. Kojima, Editors, PV 92-16, pp. 622-631, The Electrochemical Society Proceedings Series, Pennington, NJ (1992).
18. K. Zhou, T. Tekenaka, N. Sato, and M. Nanjo, *Denki Kagaku*, **59**, 981 (1991).
19. F. Lantelme, Y. Berghoute, J. H. von Barner, and G. S. Picard, *This Journal*, **142**, 4097 (1995).
20. H. A. Hjuler, A. Mahan, J. H. von Barner, and N. J. Bjerrum, *Inorg. Chem.*, **21**, 402 (1982).
21. F. Matthiesen, E. Christensen, J. H. von Barner, and N. J. Bjerrum, *This Journal*, **143**, 1793 (1996).
22. Southampton Electrochemistry Group, *Instrumental Methods in Electrochemistry*, Ellis Horwood, West Sussex, England (1990).
23. A. Salmi, Y. Berghoute, and F. Lantelme, *Electrochim. Acta*, **40**, 403 (1995).
24. T. B. Massalski, *Binary Alloy Phase Diagrams*, American Society for Metals, Materials Park, OH (1986).
25. Y. Berghoute, Ph.D. Thesis, Université Paris VI (1993).
26. R. Quigley, P. A. Barnard, C. L. Hussey, and K. R. Seddon, *Inorg. Chem.*, **31**, 1255 (1992).
27. A. Bard and L. R. Faulkner, *Electrochemical Methods: Fundamentals and Applications*, p. 232, John Wiley & Sons, Inc., New York (1980).
28. Y. Seaki and T. Suzuki, *J. Less-Common Met.*, **9**, 362 (1965).
29. T. Suzuki, *Electrochim. Acta*, **15**, 127 (1970).
30. L. Ramalay and M. S. Krause, *Anal. Chem.*, **41**, 1362 (1969).
31. J. H. Christie, J. A. Turner, and R. A. Osteryoung, *ibid.*, **49**, 1899 (1977).
32. J. O'Dea, J. Osteryoung, and R. A. Osteryoung, *ibid.*, **53**, 695 (1981).
33. J. H. von Barner, R. W. Berg, Y. Berghoute, and F. Lantelme, *Molten Salt Forum*, **1-2**, 121 (1993).
34. J. H. von Barner, E. Christensen, N. J. Bjerrum, and G. Gilbert, *Inorg. Chem.*, **30**, 561 (1991).

Electrodeposition of Zn-Ni Alloys in Sulfate Electrolytes

I. Experimental Approach

F. J. Fabri Miranda,[a] O. E. Barcia,[b,c] O. R. Mattos,*[,c] and R. Wiart[d]

[a]*Centro de Pesquisa e Desenvolvimento da Usiminas, Ipatinga, MG, Brazil*
[b]*Departamento de Fisico-Quimica-IQ/UFRJ, Rio de Janeiro, Brazil*
[c]*Laboratoire de Corrosão Professor Manuel de Castro, PEMM/COPPE/UFRJ, Rio de Janeiro, Brazil*
[d]*UPR15 CNRS, Physique des Liquides et Électrochimie, Université Pierre et Marie Curie, 75252 Paris Cedex 05, France*

ABSTRACT

The mechanism of Zn-Ni alloy deposition in acidic sulfate electrolytes is analyzed essentially from polarization curves and impedance plots, using a rotating disk electrode. The anomalous deposition of the zinc-rich phases γ and δ occurs at high cathodic polarizations, nickel deposition being inhibited and zinc deposition being stimulated. At low polarizations, nickel-rich deposits are formed, on which the diffusion-controlled hydrogen evolution predominates, at pH 1.5. The transition is shown to be related with both an increase in the interfacial pH and the presence of sulfur in the deposit. Impedance data reveal the reversibility of the charge-transfer reactions involved in hydrogen evolution and in anomalous deposition. They also show the existence of four relaxation processes: one inductive process due to zinc deposition, and three capacitive processes associated to nickel deposition and hydrogen evolution on a nickel-rich surface. They also reflect the anion adsorption.

Introduction

In recent years, great interest has been shown in the possibilities offered by the electrodeposition of alloys, mainly in the automotive industry. In particular it is known that the mechanical properties (hardness, stamping) of zinc electrodeposits can be improved by alloying zinc with nickel.[1-3] Using Zn-Ni alloy deposits on iron sheets also increases their corrosion resistance.[4-10]

The electrodeposition of Zn-Ni alloys is generally anomalous.[11] However under certain conditions (low current density), it is possible to produce normal deposition where nickel is deposited preferentially to zinc. Then a transition current density has to be reached in order to start anomalous deposition.[7]

Up to now, the codeposition mechanisms of zinc and nickel have not been well elucidated.[12,13] Various theoretical approaches have been proposed for the anomalous codeposition of Zn-Ni alloys. The first one attributes the anomalous codeposition to a local pH increase able to induce zinc hydroxide precipitation which inhibits nickel deposition.[14-16] Such a theory raises questions to account for the following points: (*i*) the proton reduction, which is important during normal codeposition, considerably vanishes during anomalous codeposition where the current efficiency is much higher, close to 98% and (*ii*) the nickel content in the alloy raises with increasing pH.[17,18]

The second theory is based on the underpotential deposition (upd) of zinc on nickel-rich zinc alloys or on nickel nuclei.[19,20] This approach does not predict the existence of a transition current density, and it hardly explains how a high zinc content in thick alloy deposits can be generated by the upd of zinc monolayers.

It can be admitted that both zinc hydroxide precipitation and zinc upd take place on the electrode surface, but these two phenomena do not suffice to account for the presence of four time-constants in the faradaic impedance of Zn-Ni alloys deposition in sulfate electrolytes, as recently reported.[21] Electrochemical impedance measurements have already given new informations on the reaction mechanism of Zn-Ni alloys deposition in chloride electrolytes[18]: a reaction model has been proposed, involving several adsorbed intermediates, and where the presence of a mixed surface compound ($ZnNi^{+}_{ad}$) governs the deposition of zinc-rich alloys. This compound, which acts as a catalyst for nickel deposition, is incorporated in the alloy deposit with increasing polarization, thus allowing zinc deposition to predominate.

The aim of this work was to investigate the mechanism of Zn-Ni alloy deposition in sulfate electrolytes. The results of the experimental approach, based essentially on

* Electrochemical Society Active Member.